

# Matter wave interferometry in a double well on an atom chip

T. Schumm,<sup>1,2</sup> S. Hofferberth,<sup>1</sup> L. M. Andersson,<sup>1</sup> S. Wildermuth,<sup>1</sup>  
S. Groth,<sup>1,3</sup> I. Bar-Joseph,<sup>3</sup> J. Schmiedmayer,<sup>1</sup> and P. Krüger<sup>1,\*</sup>

<sup>1</sup>*Physikalisches Institut, Universität Heidelberg, D-69120 Heidelberg, Germany*

<sup>2</sup>*Laboratoire Charles Fabry de l'Institut d'Optique, F-91403 Orsay Cedex, France*

<sup>3</sup>*Department of Condensed Matter Physics, The Weizmann Institute of Science, Rehovot 76100, Israel*

(Dated: May 24, 2019)

We present a coherent beam splitter on an atom chip. A one-dimensional Bose-Einstein condensate trapped in a tight magnetic trap can be split into two by means of an adiabatic radio frequency induced potential. By interfering the condensates we show that the splitting process preserves the relative phase between the two BECs even when they are split far enough to inhibit tunnel coupling.

Interferometry with matter waves [1, 2] has a great variety of applications ranging from fundamental studies of decoherence to high precision sensors [3]. Controlling and engineering complex quantum states on a microscale has been a long standing goal [4]. Here, we demonstrate an interferometer based on a novel and simple quantum beam splitter for Bose-Einstein condensates (BECs) on an atom chip. We show that this beam splitter is phase preserving and hence we demonstrate coherent quantum operation on the atom chip. The relative phase between the split BECs is measured by analysing interference patterns formed after combining the two clouds in time-of-flight expansion [5]. We have also measured the deterministic phase evolution during and after the splitting process.

At the centre of our interference experiments is the beam splitter. It is based on radio frequency induced adiabatic potentials [6, 7]. This technique has the advantage of allowing a smooth transition from a single trap into a double well potential and hence coherent splitting is possible. In contrast to other methods, the splitting distance can be orders of magnitude smaller than the chip structures. We precisely control the splitting of condensates over a range from 3-80  $\mu\text{m}$ . Our new technique allows to construct versatile chip based atom interferometers.

The combination of well established tools for atom cooling and manipulation with state-of-the-art microfabrication technology has led to the development of *atom chips* [4, 8, 9, 10, 11]. Such devices have been demonstrated to be capable of trapping and guiding ultracold atoms on a microscale. A variety of complex manipulation potentials have been formed using magnetic, electric and optical fields. BECs can be created efficiently in such microtraps and recently coherent quantum phenomena such as internal state Rabi oscillations [12] and coherent splitting in momentum space have been observed [13, 14].

It is of particular interest to control the *external* (motional) degrees of freedom of the atoms on a quantum level [15, 16]. A generic configuration for studies of matter wave dynamics is a double well potential [17]. Furthermore, dynamically splitting a single trap into a double well is analogous to a beam splitter in optics and

hence forms the basic element of an atom interferometer. Interferometers on a microchip can be employed as highly sensitive devices as they allow to measure quantum phases. This gives access to experiments studying the intrinsic phase dynamics in complex interacting quantum systems (e.g. Josephson oscillations [17, 18]) or the influence of the coupling to an external 'environment' (decoherence [19]). Technologically, chip based atom interferometers promise to be very useful as inertial sensors on a microscale [20].

Several atom chip beam splitter configurations have been proposed and experimentally demonstrated [21, 22, 23, 24], none of which could be shown to preserve the phase, i.e. to coherently split matter waves. In this work, we present a novel and easily implementable scheme for a coherent matter wave beam splitter. Our scheme is based on a combination of static and radio frequency (RF) magnetic fields. The beam splitter is fully integrated on the atom chip, as these fields are provided by microfabricated wires. By slowly changing the parameters of the RF current we can smoothly transform a tight magnetic trap into a double well and thereby dynamically split a BEC. We accurately control the splitting distance over a wide range. The potential barrier between the two wells can be raised gradually with high precision, thus enabling access to the tunnelling regime [17] as well as to the regime of entirely isolated wells. We complete an interferometer sequence and measure the relative phase between the split BECs by recombining the clouds in time-of-flight expansion. In our experiments we find an interference pattern with a fixed phase as long as the two wells are not completely separated. The phase starts to evolve deterministically once the wells are entirely separated so that tunnelling is fully inhibited on all experimental time scales.

Figure 1 illustrates the operation principle of the beam splitter. A standard magnetic microtrap [4] is formed by passing a current through a wire. In combination with an external bias field a static magnetic field minimum forms where atoms in low field seeking states can be trapped. An additional RF field generated by an independent wire carrying an alternating current couples internal atomic

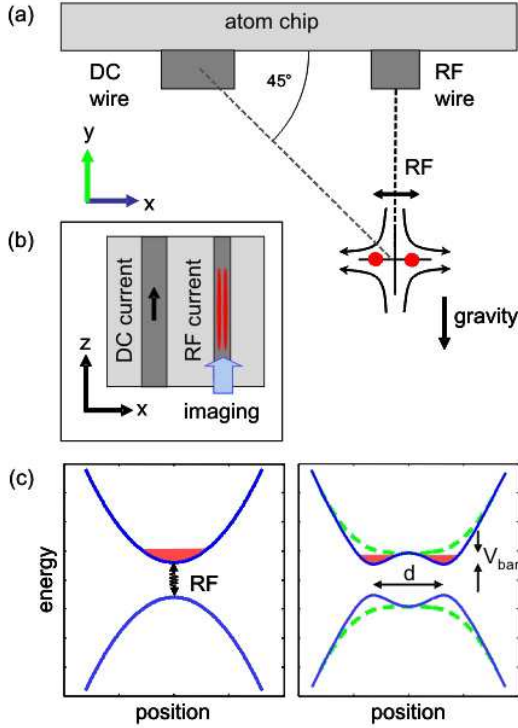


FIG. 1: Operation principle of the beam splitter. (a) A straight wire carrying a static (DC) current ( $\sim 1$  A) is used to trap a BEC on an atom chip directly above a second wire carrying a radio frequency (RF) current ( $\sim 60$  mA at 500 kHz). Placing the trap at the indicated position allows symmetric horizontal splitting. (b) Top view onto the atom chip (mounted upside down in the experiment): An elongated BEC is transversely split. All experimental images are taken along the direction parallel to the wires. (c) Left: The RF magnetic field couples different atomic spin states (only two shown for simplicity). Right: An RF frequency below the Larmor frequency at the trap minimum ( $\sim 1$  G) only relaxes the trapping potential in both transverse directions (dashed line) as long as the orientation of the RF field is orthogonal to the trapping field. An RF field oriented along  $x$  breaks the rotational symmetry of the trap, as its angle with the local static field varies along  $x$ , while along  $y$  this angle is always  $90^\circ$ . This leads to a spatially varying coupling strength which can be exploited to form a double well potential along  $x$  (solid blue line) while there is no splitting along  $y$  (dashed green line). By adjusting the RF amplitude and/or frequency, a single well can smoothly (adiabatically) be transformed into a double well allowing for coherent splitting of a condensate. Double well potentials can be formed both for RF frequencies below and above the Larmor frequency.

states with different magnetic momenta. The system can be described by a Hamiltonian with new uncoupled adiabatic eigenstates, so called *dressed states*. For sufficiently strong amplitudes of the RF field, transitions between the adiabatic levels are inhibited as the strong coupling induces large level repulsion. It has been suggested to exploit this property of the combined static and RF fields to form trapping geometries in the effective potential felt

by the dressed eigenstates [6]. Related demonstration experiments with thermal atoms in a toroidally shaped trap have been performed [7]. In our scheme we are able to form a three dimensionally confining trap with a double well shape in one of the transverse strongly confined directions. Here it is relevant that not only intensity and frequency, but also the orientation of the RF field determine the effective potential. The angle between the RF field and the local static magnetic field varies spatially, resulting in a corresponding variation of the RF coupling strength. The adiabatic potential is given by

$$V_{\text{eff}}(\mathbf{r}) = \sqrt{[\mu_m B_{\text{DC}}(\mathbf{r}) - m_F \hbar \omega_{\text{RF}}]^2 + [\mu_m B_{\text{RF}\perp}(\mathbf{r})/2]^2} \quad (1)$$

where  $\mu_m = \mu_B m_F g_F$  is the magnetic moment of the ('undressed') spin state ( $\mu_B$  is the Bohr magneton,  $m_F$  is the magnetic quantum number of the state and  $g_F$  is the Landé factor),  $B_{\text{DC}}$  is the magnitude of the static trapping field and  $\omega_{\text{RF}}$  is the frequency of the RF field.  $B_{\text{RF}\perp}$  is the magnitude of the component of the RF field perpendicular to the local direction of the static trapping field. The directional dependence of this term implies the relevance of the vector properties of the RF magnetic field which enables the formation of a true double well potential. The use of chip wire structures allows to create sufficiently strong RF fields with only moderate currents and permits precise control over the orientation of the RF field. Note that in our configuration the magnetic near field part of the RF completely dominates at the present distances and frequencies involved.

As described elsewhere [25], we routinely prepare BECs of up to  $10^5$  rubidium-87 atoms in the  $F = m_F = 2$  state in microtraps near the surface of an atom chip. Our smooth micro wires [26] enable us to create pure quasi one-dimensional condensates (aspect ratio 400) with chemical potential  $\mu \approx \hbar \omega_{\perp}$  in a trap with high transverse confinement ( $\omega_{\perp} = 2 \times 2.1$  kHz) [27, 28]. These BECs are located directly above an auxiliary wire (Figure 1). A small sinusoidally alternating current through this wire provides the RF field that splits the trap. For small splitting distances ( $< 6 \mu\text{m}$ ) we ramp the amplitude of the RF current (typically 60–70 mA) at a constant RF frequency ( $\sim 500$  kHz) to smoothly split a BEC confined in the single well trap into two. The splitting is performed transversely to the long axis of the trap, as shown in Figure 1b. The distance between the two wells can be further increased by additionally raising the frequency of the RF field (up to 4 MHz). Unbalanced splitting can occur due to the spatial inhomogeneity of the RF field, due to asymmetries in the static magnetic trap and due to gravity. The influence of gravity can be eliminated by splitting the trap horizontally (orthogonal to gravity). In the experiment we balance the double well by fine tuning the position of the original trap rel-

ative to the RF wire. The split cloud is detected by *in situ* absorption imaging along the weak trapping direction. We are able to split BECs over distances of up to  $80\text{ }\mu\text{m}$  without significant loss or heating. The measured splitting distances are in very good agreement with the theoretical expectation for different gradients of the initial single well (Figure 2).

There are a number of advantages of our beam splitter concept over previously implemented ones: The splitting distances are not limited by the structure size on the chip, but rather by the ground state size of the initial single well trap that can be orders of magnitude smaller. This allows us to reach full splitting of a BEC at a double well separation of only  $3.4\text{ }\mu\text{m}$  using a trapping wire of a width of  $50\text{ }\mu\text{m}$  at a distance of  $80\text{ }\mu\text{m}$  from the surface. Furthermore, the dynamic splitting process can be performed in a smooth (adiabatic) fashion by simply controlling the parameters of the RF field. We recombine the split clouds in time-of-flight expansion after a non-adiabatically fast extinction of the double well potential. Typical matter wave interference patterns obtained by taking absorption images 14 ms after releasing the clouds are depicted in Figure 2. The integrated transverse density profile derived from these images contains information on both the distance  $d$  of the BECs in the double well potential and the relative phase  $\Phi$  of the two condensates. We determine the fringe spacing  $\Delta z$  and the phase  $\Phi$  by fitting a cosine function with a Gaussian envelope to the measured profiles (Figure 3). For large splittings ( $d > 5\text{ }\mu\text{m}$  for our experimental parameters), the fringe spacing is given by  $\Delta z = \hbar t / md$ , where  $\hbar$  is Planck's constant,  $t$  is the expansion time and  $m$  is the atomic mass. This approximation of a non-interacting gas expanding from two point sources is inaccurate for smaller splittings where the (repulsive) interaction in the BEC has to be taken into account [29]. Figure 2 shows the observed fringe spacing that is compared to the above approximation and to a numerical integration of the time-dependent Gross-Pitaevskii equation. Again, we find excellent agreement.

The observed differential phases  $\Delta\Phi$  in the interference patterns are non-random. Hence, the splitting process is phase preserving and coherence is maintained. The differential phase spread  $\Delta\Phi$  is smaller than  $50^\circ$  for splittings of up to  $3.7\text{ }\mu\text{m}$  (Figure 3). When separating the clouds further, the phase distribution remains non-random up to at least  $d = 6\text{ }\mu\text{m}$ . An increase in phase spread and a coinciding loss of average contrast can be attributed to longitudinal phase diffusion inside the individual one-dimensional quasi BECs [30].

Determining the phase distribution at different stages of the splitting procedure, we observe that the relative phase is locked to zero, as long as the chemical potential exceeds the potential barrier; for trap separations larger than  $3.4\text{ }\mu\text{m}$ , the potential barrier is sufficiently high to suppress tunnelling. We observe a deterministic phase

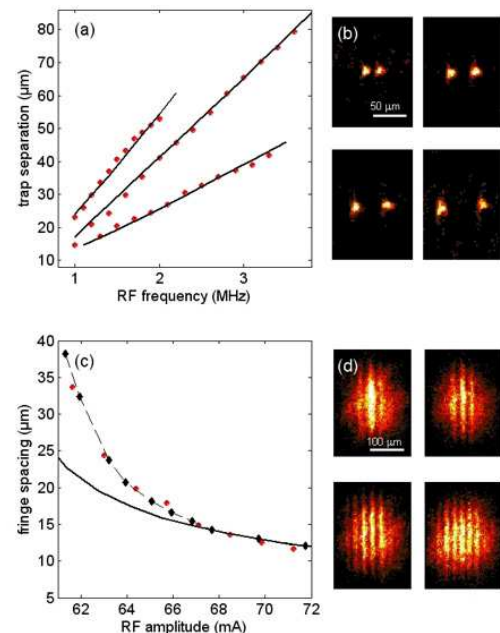


FIG. 2: The splitting of BECs is controlled over a wide spatial range. By adjusting amplitude and frequency of the RF field, we have been able to reach splitting distances of up to  $80\text{ }\mu\text{m}$ . (a) A comparison of the measured splitting distances (red circles) to the theoretical expectation (black lines) yields good agreement for three different trap configurations. (b) The experimental data is derived from *in situ* absorption images. (d) For distances below our imaging resolution ( $d < 6\text{ }\mu\text{m}$ ), we derive the splitting distances from interference patterns obtained after 14 ms potential-free time-of-flight expansion of the two BECs. (c) The fringe spacing is plotted as a function of RF amplitude (red circles). A simple approximation of the expected fringe spacing based on an expansion of a non-interacting gas from two points located at the two minima of the double well potential agrees well with the data for sufficiently large splittings (solid line). For small splitting distances (large fringe spacing), inter-atomic interactions affect the expansion of the cloud. A numerical integration of the time-dependent Gross-Pitaevskii equation using our experimental parameters takes this effect into account (black diamonds). We find good agreement to this theory. The original single well trap had a transverse oscillation frequency of  $2\pi \times 2.1\text{ kHz}$ .

shift after the splitting is complete (Figure 3). This differential phase evolution is induced by a slight residual imbalance of the double well potential (energy difference on the order of  $\hbar \times 1\text{ kHz}$  or, equivalently,  $\mu_B \times 1\text{ mG}$ ).

In conclusion, we have demonstrated coherent splitting and interference of Bose-Einstein condensates using an atom chip. Our experiments are based on a novel and versatile microfabricated beam splitter which is fully integrated on the chip. With our interferometer we have measured the phase evolution between two condensates gradually split over increasingly large distances. We are convinced that simple and robust atom chip beam split-

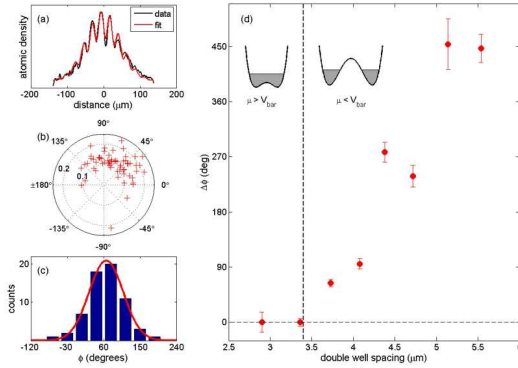


FIG. 3: The differential phase between the two split BECs is determined from interference patterns. (a) A cosine function with a Gaussian envelope is fitted to the obtained profiles yielding information on fringe spacing, contrast, and phase. (b) Contrast and phase for 82 realizations of the same experiment are plotted in a polar diagram for a double well splitting of  $3.7\mu\text{m}$ . (c) A histogram of the measured differential phase shows a Gaussian distribution around a phase shift of  $66^\circ$ . The barrier between the wells suppresses tunnel coupling completely. The width of the distribution ( $\sigma = 46^\circ$ ) is significantly narrower than for a random phase. (d) Phase evolution during the splitting process (error bars indicate the statistical error of the mean of the distribution). The dashed vertical line indicates the splitting distance at which the chemical potential  $\mu$  of the BEC is equal to the potential barrier height  $V_{\text{bar}}$ . As long as the barrier between the two wells is too low to prevent tunnel coupling (to the left of the dashed line), the relative phase remains locked at zero. Once the wells are fully separated (to the right of the dashed line), the differential phase starts to evolve due to a residual slight imbalance in the double well potential. The clouds were split at a rate of  $\sim 2\mu\text{m}/\text{ms}$ . Phase diffusion within the quasi one-dimensional BECs used in our experiments is predicted to occur on the same timescale [30]; this explains a reduction of contrast and increasing phase spread as the splitting distance is increased.

ters and interferometers based on our scheme can be the building block for quantum information experiments on the atom chip [31]. Furthermore, issues related to low dimensional correlated quantum systems can be addressed as well as applications in atom surface interactions and the fundamental question of surface induced decoherence. Microscopic atom interferometers provide also highly attractive perspectives for precision metrology.

We thank H. Perrin and I. Lesanovsky for useful discussions. We acknowledge financial support from the European Union, contract numbers IST-2001-38863 (ACQP), HPRN-CT-2002-00304 (FASTNet), HPMF-CT-2002-02022, and HPRI-CT-1999-00114 (LSF) and the Deutsche Forschungsgemeinschaft, contract number SCHM 1599/1-1.

\* Electronic address: krueger@physi.uni-heidelberg.de;  
URL: <http://www.atomchip.net>

- [1] P. Berman, ed., *Atom Interferometry*, vol. 37 of *Adv. At. Mol. Opt. Phys.* (Academic Press, New York, 1997).
- [2] G. Badurek, H. Rauch, and A. Zeilinger, eds., *Matter Wave Interferometry* (North Holland Physics Publishing Division, Amsterdam, 1988).
- [3] M. Kasevich and S. Chu, *Phys. Rev. Lett.* **67**, 181 (1991).
- [4] R. Folman, P. Krüger, J. Schmiedmayer, J. Denschlag, and C. Henkel, *Adv. At. Mol. Opt. Phys.* **48**, 263 (2002).
- [5] Y. Shin, M. Saba, T. A. Pasquini, W. Ketterle, D. E. Pritchard, and A. E. Leanhardt, *Phys. Rev. Lett.* **92**, 150401 (2004).
- [6] O. Zobay and B. M. Garraway, *Phys. Rev. Lett.* **86**, 1195 (2001).
- [7] Y. Colombe, E. Knyazchyan, O. Morizot, B. Mercier, V. Lorent, and H. Perrin, *Europhys. Lett.* **67**, 593 (2004).
- [8] D. Müller, D. Z. Anderson, R. J. Grow, P. D. D. Schwindt, and E. A. Cornell, *Phys. Rev. Lett.* **83**, 5194 (1999).
- [9] J. Reichel, W. Hänsel, and T. W. Hänsch, *Phys. Rev. Lett.* **83**, 3398 (1999).
- [10] R. Folman, P. Krüger, D. Cassettari, B. Hessmo, T. Maier, and J. Schmiedmayer, *Phys. Rev. Lett.* **84**, 4749 (2000).
- [11] N. H. Dekker, C. S. Lee, V. Lorent, J. H. Thywissen, S. P. Smith, M. Drndić, R. M. Westervelt, and M. Prentiss, *Phys. Rev. Lett.* **84**, 1124 (2000).
- [12] P. Treutlein, P. Hommelhoff, T. Steinmetz, T. W. Hänsch, and J. Reichel, *Phys. Rev. Lett.* **92**, 203005 (2004).
- [13] Y.-J. Wang, D. Z. Anderson, V. M. Bright, E. A. Cornell, Q. Diot, T. Kishimoto, M. Prentiss, R. A. Saravanan, S. R. Segal, and S. Wu, *Phys. Rev. Lett.* **94** (2005).
- [14] A. Guenther, S. Kraft, M. Kemmler, D. Koelle, R. Kleiner, C. Zimmermann, and J. Fortagh (2005), cond-mat/0504210.
- [15] T. Calarco, E. A. Hinds, D. Jaksch, J. Schmiedmayer, J. I. Cirac, and P. Zoller, *Phys. Rev. A* **61**, 022304 (2000).
- [16] E. Charron, E. Tiesinga, F. Mies, and C. Williams, *Phys. Rev. Lett.* **88**, 077901 (2002).
- [17] M. Albiez, R. Gati, J. Fölling, S. Hunsmann, M. Cristiani, and M. K. Oberthaler, *Phys. Rev. Lett.* **95**, 010402 (2005).
- [18] B. D. Josephson, *Physics Letters* **1**, 251 (1962).
- [19] W. H. Zurek, *Rev. Mod. Phys.* **75**, 715 (2003).
- [20] M. Kasevich, *Science* **298**, 1363 (2002).
- [21] D. Cassettari, B. Hessmo, R. Folman, T. Maier, and J. Schmiedmayer, *Phys. Rev. Lett.* **85**, 5483 (2000).
- [22] P. Krüger, X. Luo, M. W. Klein, K. Brugger, A. Haase, S. Wildermuth, S. Groth, I. Bar-Joseph, R. Folman, and J. Schmiedmayer, *Phys. Rev. Lett.* **91**, 233201 (2003).
- [23] D. Müller, E. A. Cornell, M. Prevedelli, P. D. D. Schwindt, A. Zozulya, and D. Z. Anderson, *Opt. Lett.* **25**, 1382 (2000).
- [24] Y. Shin, C. Sanner, G.-B. Jo, T. A. Pasquini, M. Saba, W. Ketterle, D. E. Pritchard, M. Vengalattore, and M. Prentiss (2005), cond-mat/0506464.
- [25] S. Wildermuth, P. Krüger, C. Becker, M. Brajdic, S. Haupt, A. Kasper, R. Folman, and J. Schmiedmayer, *Phys. Rev. A* **69**, 030901(R) (2004).

- [26] S. Groth, P. Krüger, S. Wildermuth, R. Folman, T. Fernholz, D. Mahalu, I. Bar-Joseph, and J. Schmiedmayer, *Appl. Phys. Lett.* **85**, 2980 (2004).
- [27] P. Krüger, L. M. Andersson, S. Wildermuth, S. Hofferberth, E. Haller, S. Aigner, S. Groth, I. Bar-Joseph, and J. Schmiedmayer (2005), *cond-mat/0504686*.
- [28] S. Wildermuth, S. Hofferberth, I. Lesanovsky, E. Haller, L. M. Andersson, S. Groth, I. Bar-Joseph, P. Krüger, and J. Schmiedmayer, *Nature* **435**, 440 (2005).
- [29] A. Röhl, M. Naraschewski, A. Schenzle, and H. Wallis, *Phys. Rev. Lett.* **78**, 4143 (1997).
- [30] N. K. Whitlock and I. Bouchoule, *Phys. Rev. A* **68**, 053609 (2003).
- [31] M. A. Cirone, A. Negretti, T. Calarco, P. Krüger, and J. Schmiedmayer (2005), published online DOI: 10.1140/epjd/e2005-00175-8.